Multi-Phase Model Update for System Identification of PSC Girders under Various Prestress Forces

Ho, Duc-Duy* Hong, Dong-Soo** Kim, Jeong-Tae†

Abstract

This paper presents a multi-phase model update approach for system identification of prestressed concrete (PSC) girders under various prestress forces. First, a multi-phase model update approach designed on the basis of eigenvalue sensitivity concept is newly proposed. Next, the proposed multi-phase approach is evaluated from controlled experiments on a lab-scale PSC girder for which forced vibration tests are performed for a series of prestress forces. On the PSC girder, a few natural frequencies and mode shapes are experimentally measured for the various prestress forces. The corresponding modal parameters are numerically calculated from a three-dimensional finite element (FE) model which is established for the target PSC girder. Eigenvalue sensitivities are analyzed for potential model-updating parameters of the FE model. Then, structural subsystems are identified phase-by-phase using the proposed model update procedure. Based on model update results, the relationship between prestress forces and model-updating parameters is analyzed to evaluate the influence of prestress forces on structural subsystems.

Keywords : *multi-phase, model update, system identification, PSC girder, prestress force*

1. Introduction

During the last decade, the development of methodology for accurate and reliable condition assessment of civil structures has become increasingly important. In structural engineering analysis and design, the finite element (FE) analysis is a powerful and useful tool to simulate the behavior of real structures. Hence, an accurate FE model is prerequisite for civil engineering applications such as damage detection, health monitoring and structural control. For complex structures, however, it is not easy to generate accurate FE models, because structural geometries, material properties and boundary conditions of those structures are not completely known. For this reason, it is usual to make simplifying assumptions when modeling the structures. As a result, an initial FE model based on as-built design may not truly represent all the physical aspects of an actual structure. On the other hand, it is generally agreed that experimental results can be considered as more reliable than numerical ones due to the advances made in instrumentation and measurement techniques. Consequently, there exists an important issue that how to update the FE model using experimental results so that the numerically analyzed structural parameters match to the real experimental ones.

The discrepancies between the FE analysis and measurement results may be caused by the following factors (Kim and Stubbs, 1995; Zhang *et al.*, 2000): (1) inaccuracy in the analytical model discretization; (2) uncertainties in structural geometries, material properties and boundary conditions; (3) variations in environmental and operational conditions during measurement; and (4) errors associated with measured signals and post-processing techniques. Among these factors, the first two factors are related to the assumptions and the inputs of the FE model. Hence,

† 책임저자, 정회원・부경대학교 해양공학과 교수
Tel: 051-629-6585 ; Fax: 051-629-6590
E-mail: idis@pknu.ac.kr
* 학생회원・부경대학교 해양공학과 박사과정
** 정회원・부경대학교 해양공학과 박사후연구원

• 이 논문에 대한 토론을 2011년 2월 28일까지 본 학회에 보내주시면 2011년 4월호에 그 결과를 게재하겠습니다.

the FE model needs to be updated in order to provide the baseline model for system identification and health condition estimation of the structure. FE model update is a process of making sure that FE analysis results better reflect the measured data than the initial model. This process is conducted by first choosing the domain such as time, frequency and time-frequency domains, in which data is presented. The second step is to determine the parts of the model that are thought to have been modeled incorrectly. The third step is to formulate a function which has the parameters that are defined as design variables and that represents the difference between the measured data and the FE model predicted data. The last step is to implement optimization methods to identify parameters that minimize this function (Friswell and Mottershead, 1995; Kwon and Lin, 2004).

Many researchers have proposed model update methods for structural identification by using dynamic characteristics (Stubbs and Osegueda, 1990; Friswell and Mottershead, 1995; Zhang *et al.*, 2001; Jaishi and Ren, 2005; Yang and Chen, 2009). In general, there are two different ways for updating the FE model of a structure, non-iterative and iterative ways, depending on whether the system matrices or the structural parameters are selected for updating. Non-iterative methods are rather single-phase procedures, in which the elements of stiffness and mass matrices are directly updated. As a result, the updated matrices reproduce the measured structural modal parameters exactly but do not generally maintain structural connectivity and the corrections are not always physically meaningful. In addition, this method can not handle the situation whereby the changes in mass and stiffness matrices are coupled together. Meanwhile, iterative methods are to select the structural geometries, material properties and boundary conditions of the FE model as model-updating parameters. Once selected, the model-updating parameters are modified through iterations to minimize the differences in dynamic characteristics between numerical analysis and experimental measurements. The modification can be performed on individual or selected groups of elements. Among iterative methods, the eigensensitivity-based algorithm has become one of the most popular and effective methods (Brownjohn *et al.*, 2001; Wu and Li, 2004).

In recent years, many prestressed concrete (PSC) girder bridges have been constructed for infrastructure systems. Therefore, the interest on the safety assessment of existing PSC bridges has been increasing. For a PSC bridge girder, typical damage types are loss of prestress force (prestress-loss) in steel tendon, loss of stiffness in concrete girder, failure of support or connection and severe ambient conditions. Among them, the loss of prestress force is one of the important monitoring targets for the serviceability and safety of PSC bridges against external loads and environmental conditions (Saiidi *et al.*, 1994; Miyamoto *et al.*, 2000; Kim *et al.*, 2004; Law and Lu, 2005). The loss of prestress force occurs along the entire girder due to elastic shortening and bending of concrete, creep and shrinkage in concrete, relaxation of steel stress, friction loss and anchorage seating (Collins and Mitchell, 1991; Nawy, 1996).

The objective of this paper is to present a multi-phase model update approach for system identification of PSC girders under various prestress forces. In order to achieve the objective, the following approaches are implemented. Firstly, a multi-phase model update method designed on the basis of eigenvalue sensitivity concept is newly proposed. Secondly, the proposed multi-phase approach is evaluated from controlled experiments on a lab-scale PSC girder for which forced vibration tests are performed for a series of prestress forces. On the PSC girder, a few natural frequencies and mode shapes are experimentally measured for the various prestress forces. The corresponding modal parameters are numerically calculated from a three-dimensional FE model which is established for the target PSC girder. Eigenvalue sensitivities are analyzed for potential model-updating parameters of the FE model. Then, structural subsystems are identified phase-by-phase using the proposed model update procedure. Based on model

update results, the relationship between prestress forces and model-updating parameters is analyzed to evaluate the influence of prestress forces on structural subsystems.

2. Multi-Phase Model Update Method

2.1 Eigenvalue Sensitivity Analysis

Eigenvalue sensitivity analysis is one of effective and popular iterative methods for model update. This technique is carried out to solve an optimization problem in which the objective function is a measure for the discrepancies between the numerical and experimental modal data. The structural parameters such as material, geometric properties and boundary conditions are defined as design variables. The iterative procedure starts with the selection of a proper set of parameters for adjustment. In order to avoid physically impossible model-updating parameter values, the lower and upper bounds of the parameters should be applied. The parameters used in the initial FE model are taken as the starting point for the iteration.

An eigenvalue sensitivity analysis is performed at each iteration process by using the parameters updated from the previous iteration. The eigenvalue sensitivities can be defined approximately by (Stubbs and Osegueda, 1990; Zhang *et al.*, 2000, 2001):

$$S_{ij} = \frac{\delta\omega_i^2}{\delta p_j}\frac{p_j}{\omega_i^2} \tag{1}$$

where S_{ij} is the dimensionless sensitivity of the i^{th} eigenvalue ω_i^2 with respect to the j^{th} structural parameter p_j; δp_j is the first order perturbation of p_j which produces the variation in eigenvalue $\delta\omega_i^2$.

The fractional change in the i^{th} eigenvalue, Z_i, between two different structural systems (e.g., an analytical model and a real structure) can be defined by:

$$Z_i = \frac{\delta\omega_i^2}{\omega_i^2} \tag{2}$$

To identify the completeness of the FE model, the convergence criterion between the measured and analytical eigenvalues is set as follows:

$$|Z_i| = \left|\frac{\omega_{i,m}^2 - \omega_{i,a}^2}{\omega_{i,a}^2}\right| \le tolerance \tag{3}$$

where $\omega_{i,m}^2$ and $\omega_{i,a}^2$ are the i^{th} eigenvalues of the measured target structure and the analytical model, respectively.

2.2 Eigensensitivity-Based System Identification Method

To identify a realistic theoretical model of a structure, Stubbs and Osegueda (1990), Kim and Stubbs (1995) proposed a system identification method which is based on the concept that combines experimental and theoretical responses of the structure (Adams *et al.*, 1978). Suppose p_j^* is an unknown parameter of the j^{th} member of a structure for which M eigenvalues are known. Also, suppose p_j is a known parameter of the j^{th} member of a FE model for which the corresponding set of M eigenvalues are known. Then, relative to the FE model, the fractional structural parameter change of the j^{th} member, $\alpha_j \ge -1$, and the structural parameters are related according to the following equation:

$$p_j^* = p_j(1+\alpha_j) \tag{4}$$

The fractional structural parameter change of NE members may be obtained using the following equation:

$$\{\alpha\} = [S]^{-1}\{Z\} \tag{5}$$

where $\{\alpha\}$ is a $NE\times 1$ matrix, which is defined by Eq. (4), containing the fractional changes in structural parameters between the FE model and the target structure; $\{Z\}$ is defined as Eq. (3) and it is a $M\times 1$ matrix containing the fractional changes in eigenvalues between two systems; and $[S]$ is $M\times NE$ sensitivity matrix, which is defined by Eq. (1), relating the

fractional changes in structural parameters to the fractional changes in eigenvalues. The sensitivity matrix, $[S]$, is determined numerically in the following procedure: (1) Introduce a known severity of damage (α_j, $j=1$, NE) at j^{th} member; (2) Determine the eigenvalues of the initial FE model (ω_{io}^2, $i=1$, M); (3) Determine the eigenvalues of the damaged structure (ω_i^2, $i=1$, M); (4) Calculate the fractional changes in eigenvalues by $Z_i=\left(\omega_i^2/\omega_{io}^2-1\right)$; (5) Calculate the individual sensitivity components from $S_{ij}=Z_i/\alpha_j$; and (6) Repeat steps (2)~(5) to generate the $M\times NE$ sensitivity matrix.

Using the above theory as a basis, a single-phase model update method has been implemented to identify baseline models of structures (Kim and Stubbs, 1995; Stubbs and Kim, 1996; Kim *et al.*, 1997). The single-phase model update is carried out in three steps. First, the fractional changes in eigenvalues between the FE model and the target structure are computed. Next, the FE model is fine-tuned by first solving Eq. (5) to estimate fractional changes in structural parameters (i.e., $NE\times 1$ $\{\alpha\}$ matrix) and then solving Eq. (4) to update the structural parameters of the FE model. Finally, the whole procedure is repeated until $\{Z\}$ or $\{\alpha\}$ approach zero when the parameters of the FE model are identified. Once the baseline model is identified, its modal parameters are numerically generated by using commercial FE analysis softwares.

2.3 Multi-Phase Model Update Approach

Despite of the feasibility of the single-phase model update method, however, it should be noted that the system is ill-conditioned and Eq. (5) will not work if the number of model-updating parameters (NE) is much larger than the number of modes (M), i.e., $NE \gg M$, which is a typical situation for civil engineering structures. For this reason, the number of model-updating parameters should be equal to or smaller than the number of modes, $NE \leq M$. In addition, it is very hard to generate accurate FE models for complex structures (e.g., PSC structures), since those structures have a variety of sub-structural members which are mixed with complex motions.

In order to overcome these problems, a multi-phase model update approach is needed to be implemented for updating the FE models of complex structures. For the multi-phase model update, structural subsystems are identified by phase-by-phase model update procedures. In each phase, the selection of model-updating parameters is based on the eigenvalue sensitivity analysis and the number of available modes. Primary model-updating parameters which are more sensitive to structural responses will be updated in the prior phases. The other parameters which are less sensitive to structural responses will be updated in the following phases. In the model update procedure, the model-updating parameters should be selected very carefully, because the accuracy of the baseline model depends on the number of model-updating parameters. It is also expected that the rate of convergence be improved phase after phase, and, as a result, the accuracy of the baseline model be improved consequently.

For a target structure which has experimental modal parameters ($\phi_{i,m}$, $\omega_{i,m}^2$, $i=1$, M; where $\phi_{i,m}$ and $\omega_{i,m}^2$ are the i^{th} measured modal vector and eigenvalue, respectively), the procedure of multi-phase model update is schematized in Fig. 1. The procedure is summarized as follows:

(1) Establish an initial FE model and numerically analyze for modal parameters ($\phi_{i,a}$, $\omega_{i,a}^2$, $i=1$, M; where $\phi_{i,a}$ and $\omega_{i,a}^2$ are the i^{th} analytical modal vector and eigenvalue, respectively);

(2) Select NE model-updating parameters (p_j, $j=1$, NE) by grouping the FE model into NE sub-structures and analyzing modal sensitivities of the NE parameters up to M modes;

(3) Determine the number of phases NP by computing $NP=NE/M$ and arrange the M number of model-updating parameters (p_j, $j=1$, M) for each phase; and

(4) Perform the following six sub-steps for each

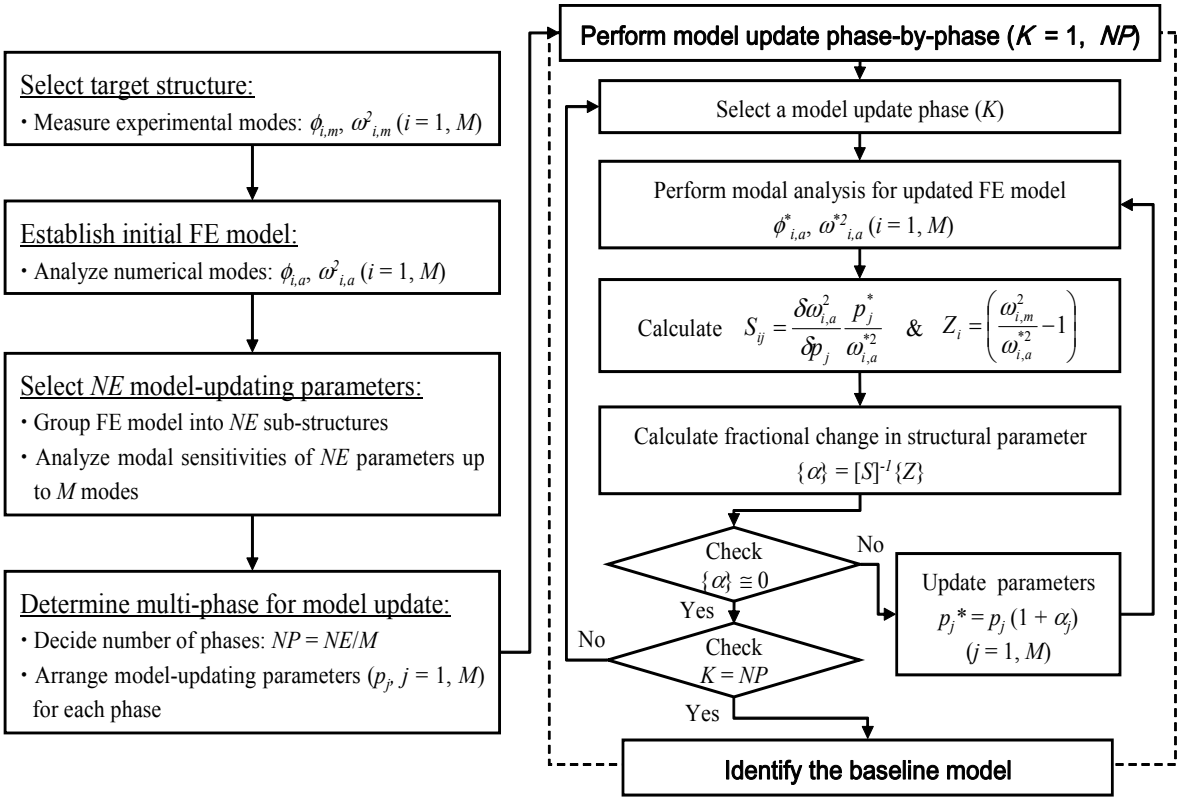

Fig. 1 Procedure of multi-phase model update method

phase (K=1, NP):

(a) Select a model update phase K;

(b) Perform modal analysis for an updated FE model ($\phi^*_{i,a}$, $\omega^{*2}_{i,a}$, i=1, M);

(c) Calculate sensitivities of the updated parameters by Eq. (1) and the fractional changes in eigenvalues between the target structure and the updated FE model by Eq. (2) as $Z_i = \left(\omega^2_{i,m}/\omega^{*2}_{i,a} - 1\right)$;

(d) Calculate Eq. (5) for the fractional change in structural parameters;

(e) Check the convergence of updated parameters and decide whether to continue updating in the phase (K) or to proceed to next phase (K+1); and

(f) Identify the baseline model after all phases are completed.

3. Forced Vibration Test on Lab-Scale PSC Girder

Dynamic tests were performed on a lab-scale post-tension PSC girder to determine the experimental modal parameters for a set of prestress cases. The structure was tested in Smart Structure engineering Lab located at Pukyong National University, Busan, Korea. During the test, temperature and humidity in the laboratory were kept close to constant as 18~19℃ and 40~45% by air conditioners, respectively, in order to minimize the effect of those ambient conditions that, if not controlled, might lead to significant changes in dynamic characteristics. The schematic of the test structure is shown in Fig. 2. The PSC girder was simply supported with the span length of 6m and installed on a rigid testing frame. Two simple supports of the girder were simulated by using thin rubber pads as interfaces between the girder and the rigid frame. The T-section was reinforced in both longitudinal and transverse direction with 10mm diameter reinforcing bars (equivalent to Grade 60). The stirrups were used to facilitate the position of the top bars. A seven-wire straight concentric mono-strand with 15.2mm diameter (equivalent to Grade 250) was used as the prestressing tendon. The tendon was placed in a 25mm diameter duct that remained

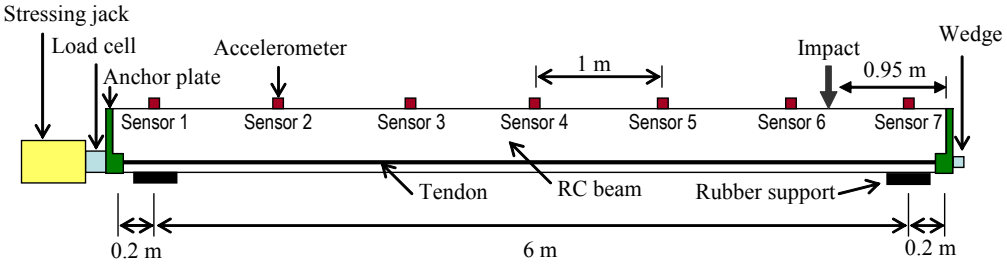

(a) Experimental setup for PSC girder

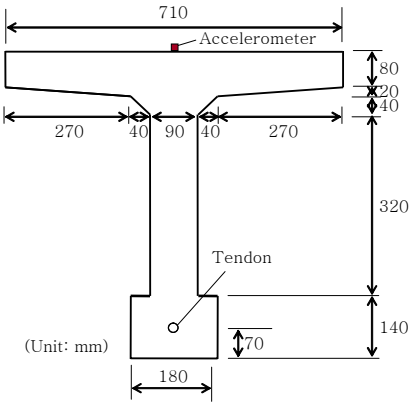

(b) Cross section

(c) Test girder

Fig. 2 Dynamic test on the lab-scale PSC girder

ungrouted.

Seven sensor locations and their arrangements on the test structure were designed as shown in Fig. 2(a). For acceleration measurement, seven accelerometers (Sensors 1~7) were placed along the girder with a constant interval 1m and the impact excitation was applied at a location 0.95m distanced from the right edge. Seven ICP-type accelerometers, PCB 393B04, with the nominal sensitivity of 1 V/g and the specified frequency range (±5%) of 0.06~450Hz were used. The accelerometers were mounted on magnetic blocks which were attached to steel washers bonded on the top surface of the girder. Impact forces were applied to the PSC girder by an impulse hammer. The data acquisition system consists of a 16-channel PXI-4472 DAQ, a PXI-8186 controller with LabVIEW (National Instruments, 2009) and MATLAB (The MathWorks Inc., 2004). Dynamic responses in vertical direction were measured by the PCB accelerometers with the sampling frequency of 300Hz. Frequency domain decomposition (FDD) technique (Brincker *et al.*, 2001; Yi and Yun, 2004) was employed to extract frequency responses and modal parameters from the acceleration signals measured at the seven sensor locations.

Axial prestress forces were introduced into the tendon by a stressing jack as the tendon was anchored at one end and pulled out at the other. A load cell was installed at the left end to measure the applied prestress force. Each test was conducted after the desired prestress force has been applied and the cable has been anchored. During the measurement, the stressing jack was removed from the girder to avoid the influence of the jack weight on dynamic characteristics of the test structure. The prestress force was applied to the test structure up to five different prestress cases (i.e., PS1-PS5). The minimum and maximum prestress forces were set to 39.2kN and 117.7kN, respectively. The prestress force was uniformly increased by 19.6kN for each prestress-loss case.

For the five prestress cases, frequency responses were extracted from acceleration signals measured at sensor 5, as shown in Fig. 3(a). Mode shapes of the first two bending modes were measured for the undamaged state of the PSC girder, as shown in Fig. 3(b). Natural frequencies of the first two bending

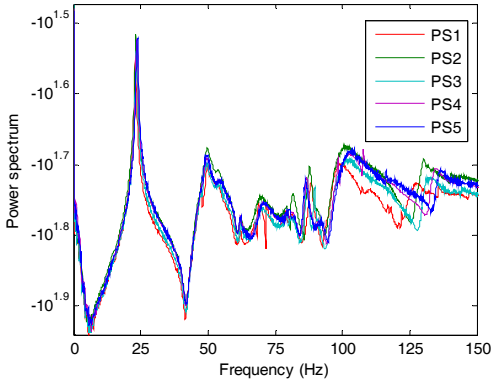

(a) Frequency responses

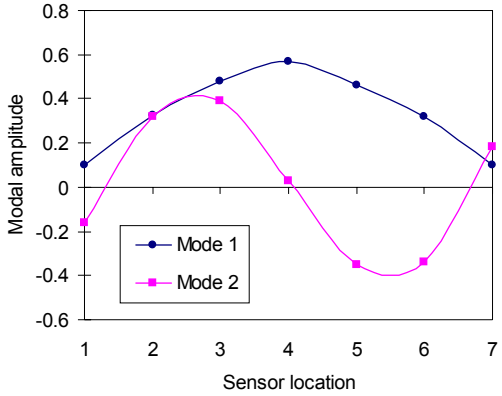

(b) Bending mode shapes

Fig. 3 Frequency responses and mode shapes from experimental measurement

Table 1 Experimental natural frequencies of test structure measured for five prestress cases

Prestress case	Prestress force(kN)	Natural frequency(Hz)	
		Mode 1	Mode 2
PS1	39.2	23.08	98.73
PS2	58.9	23.23	101.39
PS3	78.5	23.39	101.65
PS4	98.1	23.60	101.70
PS5	117.7	23.72	102.54

modes which were experimentally measured for the five prestress cases are summarized in Table 1. As also shown in Fig. 4, the natural frequencies are increased as the prestress forces are increased. In Fig. 3(a), there are several peaks between first and second bending modes. These modes may be twist modes, axial modes and horizontal bending modes. As shown in Fig. 2(a), seven accelerometers were placed in vertical direction on top of the girder. Also, the impact excitation was applied in vertical direction by an electromagnetic shaker VTS100. For this reason, only

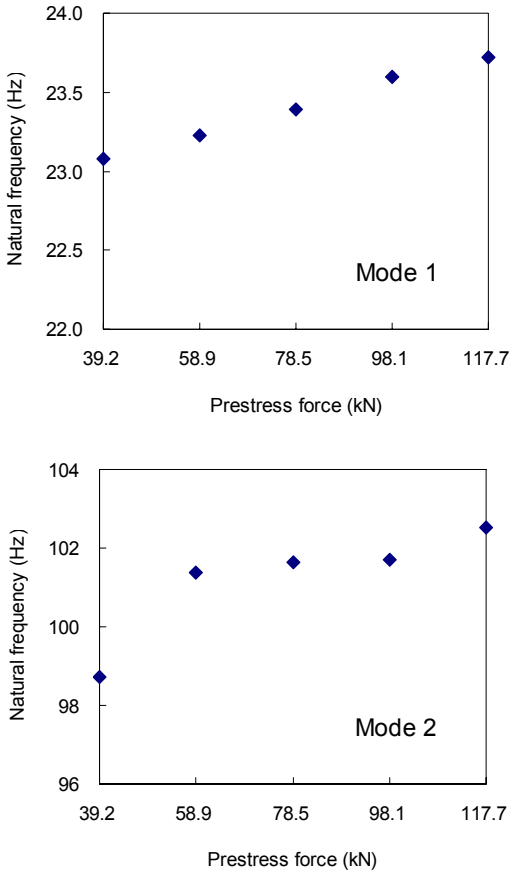

Fig. 4 Change in experimental natural frequencies for five prestress cases

vertical bending modes were extracted exactly from experimental setup.

4. Multi-Phase Model Update of PSC Girder

4.1. Initial FE Model of PSC Girder

An analytical model should be established to represent the test structure. The reliable model update depends on the accuracy of the experimental data, on assuming that the experimental modal information is error free. It should be noted that the iterative model update process may not be efficient to get the convergence when the discrepancies between experimental results and the analytical model are too large. Hence, the initial FE model should be relatively close to the experimentally measured behavior.

A structural analysis and design software, SAP2000 (Computers and Structures Inc., 2005), was used to

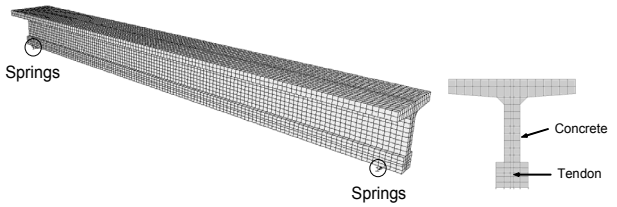

Fig. 5 Initial FE model of the PSC girder

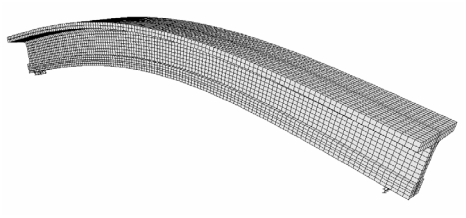

(a) Mode 1

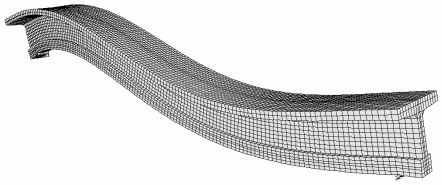

(b) Mode 2

Fig. 6 Numerical mode shapes obtained from the initial FE model

model the PSC girder. The girder was constructed by a three-dimensional FE model using solid elements. The dimensions of the FE model were the same as the real structure shown in Fig. 2. For the boundary conditions, spring restraints were assigned at the supports shown in Fig. 5. Initial values of material, geometric properties and boundary conditions of the FE model were assumed as follows: (1) for the concrete girder, elastic modulus $E_c = 2\times10^{10}\text{N/m}^2$, the second moment of area $I_c = 4.9\times10^{-3}\text{m}^4$, mass density $\rho_c = 2500\text{kg/m}^3$, and Poisson's ratio $\upsilon_c = 0.2$; (2) for the steel tendon, elastic modulus $E_p = 3\times10^{11}\text{N/m}^2$, the second moment of area $I_p = 1.9\times10^{-5}\text{m}^4$, mass density $\rho_p = 7850\text{kg/m}^3$, and Poisson's ratio $\upsilon_p = 0.3$; and (3) the stiffness of vertical and horizontal springs $k_v = k_h = 10^9\text{N/m}$. The structural dynamic analysis was performed on the initial FE model and initial natural frequencies of the first two bending modes were computed as 23.65Hz and 97.77Hz, respectively. Fig. 6 shows mode shapes of the two modes analyzed from the FE model.

4.2 Model-Updating Parameters of PSC Girder

Choosing appropriate model parameters is an important step in the FE model-updating procedure. Theoretically, all parameters related to structural geometries, material properties, and boundary conditions can be potential choices for adjustment in the model-updating procedure. However, the optimal number of parameters should be selected on the basis of their effectiveness on structural responses as much as the availability of experimental modal data. When too many parameters are selected relative to the amount of available modal data, the problem may be turned out to be ill-conditioned or at least under- determined. Therefore, the model-updating parameters should be selected on the basis of the following two facts. Physically, the parameters which are uncertain in the model due to the lack of knowledge on structural properties should be selected. Also, the parameters which are relatively sensitive to vibration responses should be selected. The modal sensitivities with respect to the main structural parameters are first calculated and then the most sensitive and insensitive parameters to the responses are examined next.

In this study, two parameters, elastic modulus (E) and second moment of area (I) should be combined as a stiffness parameter (EI) to reduce the number of model-updating parameters. Furthermore, EI has more physical meaning than E or I in structural analysis. As shown in Fig. 7, for the present PSC girder, six model-updating parameters were selected as follows: (1) flexural rigidity of concrete girder (E_cI_c) in the simple-span domain, (2) flexural rigidity of steel tendon (E_pI_p) in the overall structure, (3) vertical spring stiffness (k_v) at the left and right supports, (4) horizontal spring stiffness (k_h) at the left support, (5) flexural rigidity of the left overhang zone ($E_{lo}I_{lo}$), and (6) flexural rigidity of the right overhang zone ($E_{ro}I_{ro}$). As shown in Fig. 2(a), the left overhang zone includes stressing-jack, load-cell, tendon anchor, and 0.2m girder section at the left edge. Also, the right overhang zone includes tendon anchor and 0.2m

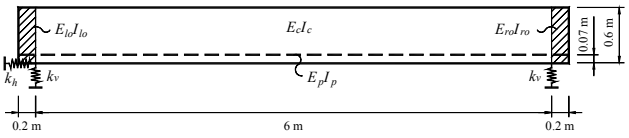

Fig. 7 Six model-updating parameters for PSC girder

girder section at the right edge. Both overhang zones were selected due to the uncertainty in the stiffness due to the lack of knowledge on the effect of tendon anchors and concrete sections on dynamic responses under varying prestress forces.

On estimating the structural geometries, material properties and boundary conditions of the initial FE model, the initial values of the selected model parameters were assumed as follows: $E_cI_c = 9.81\times 10^7 \mathrm{Nm}^2$, $E_pI_p = 5.73\times 10^6 \mathrm{Nm}^2$, $k_v = k_h = 10^9 \mathrm{N/m}$, and $E_{lo}I_{lo} = E_{ro}I_{ro} = 9.81\times 10^7 \mathrm{Nm}^2$. Then, the eigenvalue sensitivity analysis for the six model-updating parameters was carried out, as summarized in Table 2. From the results, the flexural rigidity of concrete girder was the most sensitive parameter for both mode 1 and mode 2. The flexural rigidity of steel tendon was the second sensitive parameter. Those high sensitive parameters were expected to contribute more intensively on the model update. The stiffness of support springs and the stiffness of overhang zones are relatively less sensitive parameters. That is, those less sensitive parameters were expected to contribute less intensively on the model update.

Due to the availability of the two modes, three model update phases were chosen in order to update the six model-updating parameters by two at a phase. In each phase, two model-updating parameters were chosen for adjustment. Based on their sensitivities as listed in Table 2, the order of model update was arranged as follows:

(1) Phase I (*Girder & Tendon*): flexural rigidity of concrete girder (E_cI_c) and flexural rigidity of steel tendon (E_pI_p);

(2) Phase II (*Support Springs*): vertical spring stiffness (k_v) and horizontal spring stiffness (k_h); and

(3) Phase III (*Overhang Zones*): flexural rigidity of left overhang zone ($E_{lo}I_{lo}$) and flexural rigidity of right overhang zone ($E_{ro}I_{ro}$).

Table 2 Eigenvalue sensitivities of six model-updating parameters of test structure

Mode number	Eigenvalue sensitivities					
	E_cI_c	E_pI_p	k_v	k_h	$E_{lo}E_{lo}$	$E_{ro}I_{ro}$
1	0.8855	0.1039	0.0029	0.0007	0.0064	0.0034
2	0.8817	0.0537	0.0150	0.0268	0.0223	0.0105

4.3 System Identification of PSC Girder under Various Prestress Forces

After selection of responses and parameters, an iterative procedure was carried out for model update. In this study, the baseline natural frequencies were identified by using the eigensensitivity-based multi-phase model update method described previously and also depicted in Fig. 1. According to this method, in order to quit iteration of updating phase before starting new phase, the errors of updated natural frequencies with compared to target natural frequencies for each mode should be converged. It should be noted that three phases were considered for updating two modes. These phases were updated by phase-by-phase. For each phase, two model-updating parameters were updated iteratively. Consequently, the analytical natural frequencies for both mode 1 and mode 2 determined at the end of iterations should gradually approach those experimental values.

The system identification results for prestress case PS1 (39.2kN) are summarized in Table 3 and Table 4, and also shown in Fig. 8(a). For the PS1 case, natural frequencies of the first two modes were used to update the FE model through 12 iterations. Table 3 shows natural frequencies during 12 iterations of multi-phase model update. Table 4 shows values of model parameters during 12 iterations of multi-phase model update. Also, Fig. 8(a) shows convergence errors of the natural frequencies of updated models during 12 iterations, with compared to target natural frequencies measured at the prestress force of 39.2kN. Natural frequencies of the two modes were converged within 0.6% error at Phase I, 0.4%

Table 3 Natural frequencies(Hz) during multi-phase model update for prestress case PS1 (39.2kN)

Mode number	Initial freqs. (Hz)	Updated frequencies(Hz) at each iteration												Target freqs. (Hz)
		Phase I (*Girder & Tendon*)					Phase II (*Spring Supports*)				Phase III (*Overhang Zones*)			
		1st	2nd	3rd	4th	5th	6th	7th	8th	9th	10th	11th	12th	
1	23.65	23.54	23.30	23.10	23.17	23.21	23.19	23.17	23.17	23.16	23.12	23.12	23.11	23.08
2	97.77	99.39	98.51	97.76	98.02	98.17	98.60	98.53	98.49	98.37	98.47	98.92	98.64	98.73

Table 4 Value of model-updating parameters for prestress case PS1 (39.2kN)

Model parameter	Initial value	Phase I (*Girder & Tendon*)					Phase II (*Support Springs*)				Phase III (*Overhang Zones*)			Updated value
		1st	2nd	3rd	4th	5th	6th	7th	8th	9th	10th	11th	12th	
E_cI_c(Nm^2)	9.81E+7	1.08E+8	1.06E+8	1.05E+8	1.05E+8	1.06E+8	1.06E+8	1.06E+8	1.06E+8	1.06E+8	1.06E+8	1.06E+8	1.06E+8	1.06E+8
E_pI_p(Nm^2)	5.73E+6	5.73E+5	2.87E+5	2.12E+5	2.01E+5	1.93E+5	1.93E+5	1.93E+5	1.93E+5	1.93E+5	1.93E+5	1.93E+5	1.93E+5	1.93E+5
k_v(N/m)	1.00E+9	1.00E+9	1.00E+9	1.00E+9	1.00E+9	1.00E+9	5.50E+8	4.15E+8	3.95E+8	3.68E+8	3.68E+8	3.68E+8	3.68E+8	3.68E+8
k_h(N/m)	1.00E+9	1.00E+9	1.00E+9	1.00E+9	1.00E+9	1.00E+9	3.90E+9	3.37E+10	1.64E+12	1.65E+12	1.65E+12	1.65E+12	1.65E+12	1.65E+12
$E_{lo}I_{lo}$(Nm^2)	9.81E+7	9.81E+7	9.81E+7	9.81E+7	9.81E+7	9.81E+7	9.81E+7	9.81E+7	9.81E+7	9.81E+7	2.45E+8	3.68E+8	3.90E+8	3.90E+8
$E_{ro}I_{ro}$(Nm^2)	9.81E+7	9.81E+7	9.81E+7	9.81E+7	9.81E+7	9.81E+7	9.81E+7	9.81E+7	9.81E+7	9.81E+7	9.81E+6	4.90E+6	9.81E+5	9.81E+5

Table 5 Natural frequencies (Hz) of updated FE models and target structures for five prestress cases

Mode number	PS1 (39.2kN)			PS2 (58.9kN)			PS3 (78.5kN)			PS4 (98.1kN)			PS5 (117.7kN)		
	FEM	Target	Error (%)	FEM	Target	Error (%)	FEM	Target	Error (%)	FEM	Target	Error (%)	FEM	Target	Error (%)
1	23.11	23.08	0.12	23.51	23.23	1.18	23.63	23.39	1.02	23.75	23.60	0.62	23.91	23.72	0.80
2	98.64	98.73	0.09	100.28	101.39	1.09	100.77	101.65	0.87	101.26	101.70	0.43	101.95	102.54	0.58

Table 6 Updated values of model parameters for five prestress cases

Model parameter	Initial value	Updated model parameter				
		PS1(39.2kN)	PS2(58.9kN)	PS3(78.5kN)	PS4(98.1kN)	PS5(117.7kN)
E_cI_c(Nm^2)	9.81E+7	1.06E+8	1.09E+8	1.10E+8	1.11E+08	1.12E+08
E_pI_p(Nm^2)	5.73E+6	1.93E+5	2.88E+5	3.78E+5	4.78E+05	5.75E+05
k_v(N/m)	1.00E+9	3.68E+8	3.72E+8	3.67E+8	3.71E+08	3.74E+08
k_h(N/m)	1.00E+9	1.65E+12	1.66E+12	1.64E+12	1.65E+12	1.66E+12
$E_{lo}I_{lo}$(Nm^2)	9.81E+7	3.90E+8	3.98E+8	4.01E+8	4.04E+8	4.10E+8
$E_{ro}I_{ro}$(Nm^2)	9.81E+7	9.81E+5	1.05E+6	1.13E+6	1.20E+6	1.31E+6

error at Phase II, and less than 0.12% error at the end of Phase III. Meantime, in Phase I, the flexural rigidities of concrete girder and steel tendon were identified as $E_cI_c = 1.06\times10^8$Nm^2 and $E_pI_p = 1.93\times10^5$Nm^2, respectively. In Phase II, the stiffness parameters of support springs were identified as $k_v = 3.68\times10^8$ N/m and $k_h = 1.65\times10^{12}$N/m, respectively. Also, in Phase III, the flexural rigidities of overhang zones were identified as $E_{lo}I_{lo} = 3.9\times10^8$Nm^2 and $E_{lo}I_{lo} = 9.81\times10^5$Nm^2, respectively.

The system identification results for all five cases PS1-PS5 are summarized in Table 5 and Table 6. Table 5 shows natural frequencies of updated FE models with compared to those of target structure. For all five cases, as also shown in Fig. 8, natural frequencies were converged approximately within less than 1.2% error. By utilizing the updated results of previous prestress case as the starting point for next one, the rate of convergence was improved as shown in Figs. 8(b)~(e). Meanwhile, the six parameters were identified as listed in Table 6.

4.4 Effect of Prestress Forces on Model Parameters

As listed in Table 6, the updated model parameters were changed as the prestress forces were changed from PS1 (39.2kN) to PS5 (117.7kN). Fig. 9 shows the relative changes in updated model parameters due

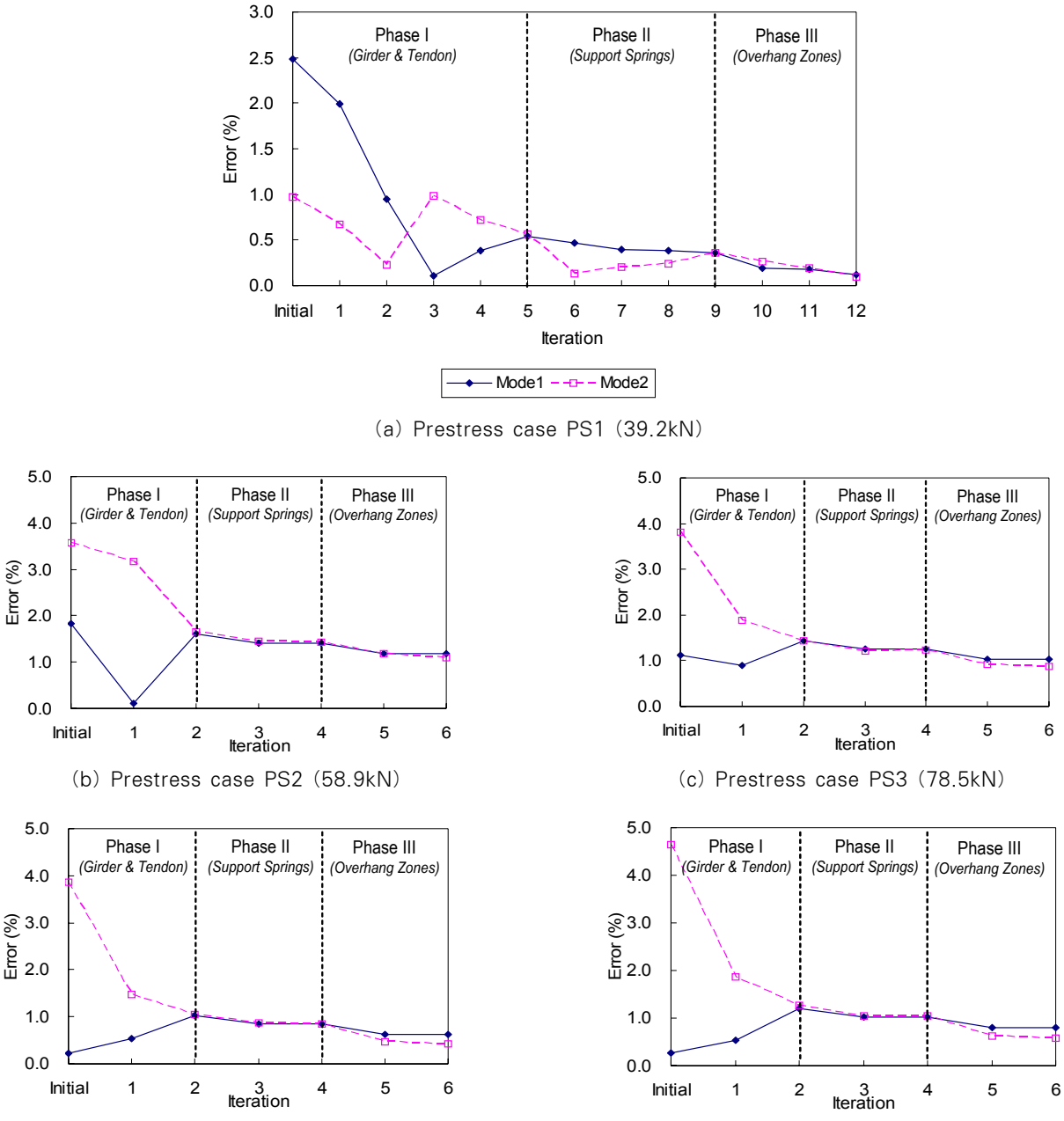

(a) Prestress case PS1 (39.2kN)

(b) Prestress case PS2 (58.9kN)

(c) Prestress case PS3 (78.5kN)

(d) Prestress case PS4 (98.1kN)

(e) Prestress case PS5 (117.7kN)

Fig. 8 Convergence errors of natural frequencies for five prestress cases

to the changes in prestress forces. Those fractional changes in model parameters were computed with respect to prestress case PS1 as the reference.

Fig. 9(a) shows the relationship between the relative change in the flexural rigidity of concrete girder ($\delta E_c I_c$) and the prestress forces. Fig. 9(b) shows the relationship between the prestress forces and the relative change in the flexural rigidity of steel tendon ($\delta E_p I_p$). It is observed that both concrete girder's stiffness and steel tendon's stiffness increase almost linearly as the prestress force increases. As prestress forces were increased, the steel tendon's stiffness was greatly increased. The change in concrete girder's stiffness was relatively small compared to the steel tendon's stiffness. Fig. 9(c) and (d) show the relationship between the prestress forces and the relative change in the vertical and horizontal spring stiffness (δk_v and δk_h). The spring's stiffness is nearly

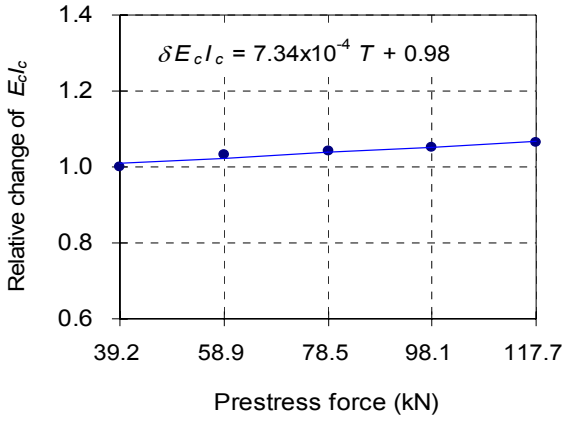

(a) Concrete girder's E_cI_c

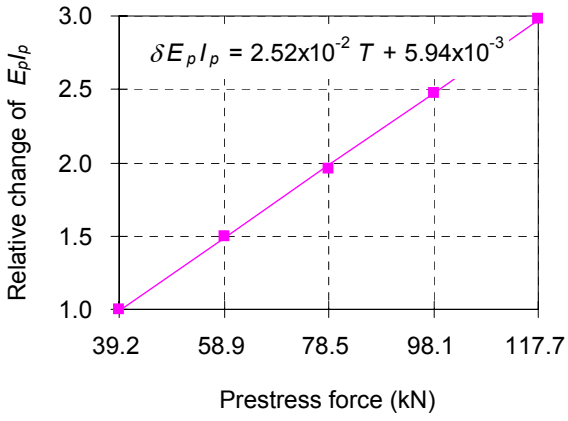

(b) Steel tendon's E_pI_p

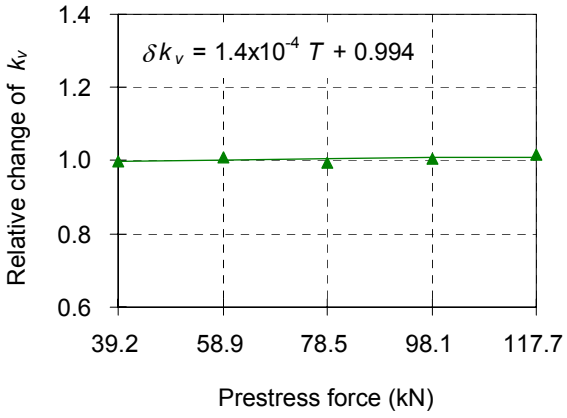

(c) Vertical spring's k_v

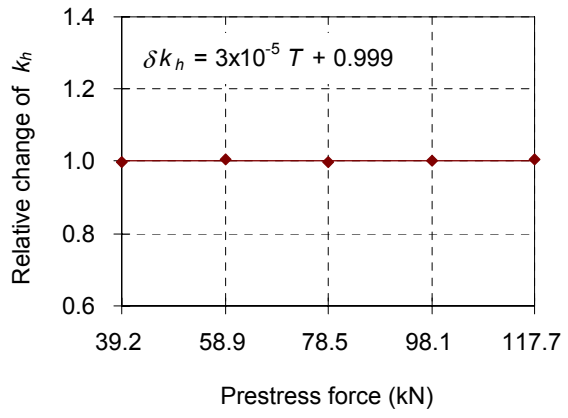

(d) Horizontal spring's k_h

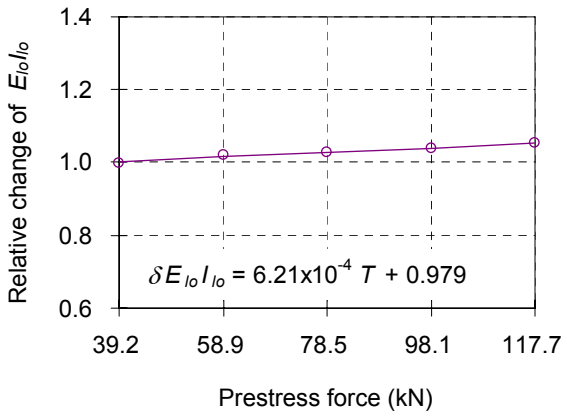

(e) Left overhang's $E_{lo}I_{lo}$

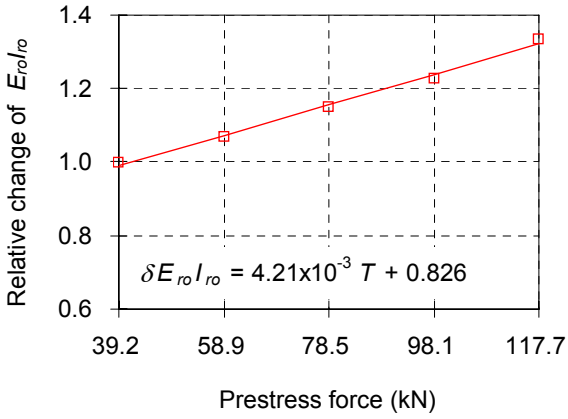

(f) Right overhang's $E_{ro}I_{ro}$

Fig. 9 Relative changes in updated model parameters due to changes in prestress forces

unchanged as the prestress force increases. Fig. 9(e) and (f) show the relationship between the prestress forces and the relative change in the left and right overhang's stiffness ($\delta E_{lo}I_{lo}$ and $\delta E_{ro}I_{ro}$). The change in the right overhang's stiffness was relatively larger than the left overhang which remained almost unchanged.

The effect of prestress forces on the model parameters can be estimated from the analysis on the relationship between prestress forces and the relative changes in model parameters. As indicated in Fig. 9, six empirical equations were established, from the linear regression analysis, to estimate the relative

change (with respect to the prestress case PS1 as the reference) in model parameters (i.e., $\delta E_c I_c$, $\delta E_p I_p$, δk_v, δk_h, $\delta E_{lo} I_{lo}$, and $\delta E_{ro} I_{ro}$ shown in Fig. 9) due to the change in prestress force T (kN) in the PSC girder. Also, from those empirical equations, values of six model parameters corresponding to certain amounts of prestress forces can be predicted as follows:

$$E_c I_c = 1.06 \times 10^8 \times \delta E_c I_c = 7.75 \times 10^4 T + 1.04 \times 10^8 \, Nm^2 \quad (6)$$

$$E_p I_p = 1.93 \times 10^5 \times \delta E_p I_p = 4.86 \times 10^3 T + 1.15 \times 10^3 \, Nm^2 \quad (7)$$

$$k_v = 3.68 \times 10^8 \times \delta k_v = 5.16 \times 10^4 T + 3.66 \times 10^8 \, N/m \quad (8)$$

$$k_h = 1.65 \times 10^{12} \times \delta k_h = 4.94 \times 10^7 T + 1.65 \times 10^{12} \, N/m \quad (9)$$

$$E_{lo} I_{lo} = 3.9 \times 10^8 \times \delta E_{lo} I_{lo} = 2.42 \times 10^5 T + 3.82 \times 10^8 \, Nm^2 \quad (10)$$

$$E_{ro} I_{ro} = 9.81 \times 10^5 \times \delta E_{ro} I_{ro} = 4.13 \times 10^3 T + 8.1 \times 10^5 \, Nm^2 \quad (11)$$

By utilizing the above equations, design values of the six model parameters may be assessed with respect to the required amount of prestress force. Also, a solid baseline model which represents dynamic responses corresponding to a certain prestress force can be analyzed in terms of the six model parameters. Finally, the identified baseline model can be the role of the reference structure to make diagnosis or prognosis on the structure of interest.

5. Summary and Conclusions

A multi-phase model update approach was developed for system identification of PSC girders under various prestress forces. In order to achieve the objective, the following approaches were implemented. First, a multi-phase model update approach designed on the basis of eigenvalue sensitivity concept was newly proposed. Next, the proposed multi-phase approach was evaluated from controlled experiments on a lab-scale PSC girder for which forced vibration tests were performed for a series of prestress forces.

On the PSC girder, the first two bending natural frequencies and mode shapes were experimentally measured for five cases of axial prestress forces which were introduced in the structure. The corresponding modal parameters were numerically calculated from a three-dimensional FE model which was established for the target PSC girder. Eigenvalue sensitivities were analyzed for six model-updating parameters which were selected for model adjustment. As a result, three phases were considered to deal with two available modes by two model-updating parameters in each phase.

From phase-by-phase identification of structural subsystems, good correlations and convergences of natural frequencies between identified FE models and target PSC girders were obtained for all five cases of prestress forces. It is also observed that updated model parameters were changed as the prestress forces were changed. From linear regression analysis of the results, the relationships between updated model parameters and prestress forces were established to predict the influence of prestress forces on the performance of structural subsystems.

Acknowledgement

This study was supported by Korean Science and Engineering Foundation (KOSEF) through Smart Infra-Structure Technology Center (SISTeC) in the program year of 2010. Also, graduate students participated in this study were supported by the 2nd Stage Brain Korea 21 (BK21) Program of Korean Government.

References

Adam, R.D., Cawley, P., Pye, C.J., Stone, B.J. (1978) A Vibration Technique for Non-Destructively Assessing the Integrity of Structures, *Journal of Mechanical Engineering Science*, 20, pp.93~100.

Brincker, R., Zhang, L., Andersen, P. (2001) Modal Identification of Output-Only Systems using Frequency Domain Decomposition, *Smart Materials and Structures*, 10, pp.441~445.

Brownjohn, J.M.W., Xia, P.Q., Hao, H., Xia, Y.

(2001) Civil Structure Condition Assessment by FE Mode Lupdating: Methodology and Case Studies, *Finite Elements in Analysis and Design*, 37, pp.761~775.

Collins, M.P., Mitchell, D. (1991) *Prestressed Concrete Structures*, Prentice Hall, Englewood Cliffs, New Jersey.

Computers and Structures Inc. (2005) *CSI Analysis Reference Manual for SAP2000*, Berkeley, USA.

Friswell, M.I., Mottershead, J.E. (1995) *Finite Element Model Updating in Structural Dynamics*, Kluwer Academic, Boston.

Jaishi, B., Ren, W.X. (2005) Structural Finite Element Model Updating using Ambient Vibration test Results, *Journal of Structural Engineering*, 131(4), pp.617~628.

Kim, J.T., Stubbs, N. (1995) Model-Uncertainty Impact and Damage-Detection Accuracy in Plate Girder, *Journal of Structural Engineering*, 121(10), pp.1409~1417.

Kim, J.T., Ryu, Y.S, Lee, B.H., Stubbs, N. (1997) Smart Baseline Model for Nondestructive Evaluation of Highway Bridges, *Proceeding of SPIE International Symposium, Smart Systems for Bridges, Structures, and Highways*, San Diego, March.

Kim, J.T., Yun, C.B., Ryu, Y.S., Cho, H.M. (2004) Identification of Prestress-Loss in PSC Beams using Modal Information, *Structural Engineering and Mechanics*, 17(3~4), pp.467~482.

Kwon, K.S., Lin, R.M. (2004) Frequency Selection Method for FRF-based Model Updating, *Journal of Sound and Vibration*, 278, pp.285~306.

Law, S.S., Lu, J.R. (2005) Time Domain Response of a Prestressed Beam and Prestress Identification, *Journal of Sound and Vibration*, 288(4~5), pp.1011~1025.

Miyamoto, A., Tei, K., Nakamura, H., Bull, J.W. (2000) Behavior of Prestressed beam Strengthened with External Tendons, *Journal of Structural Engineering*, 126, pp.1033~1044.

National Instruments (2009) www.ni.com.

Nawy, E.G. (1996) *Prestressed concrete - A Fundamental Approach*, PrenticeHall, USA.

Saiidi, M., Douglas, B., Feng, S. (1994) Prestress Force Effect on Vibration Frequency of Concrete Bridges, *Journal of Structural Engineering*, 120, pp.2233~2241.

Stubbs, N., Kim, J.T. (1996) Damage Localization in Structures Without Baseline Modal Parameters, *AIAA Journal*, 34(8), pp.1644~1649.

Stubbs, N., Osegueda, R. (1990) Global Non-Destructive Damage Evaluation in Solids, *The International Journal of Analytical and Experimental Modal Analysis*, 5(2) pp.67~79.

The MathWorks Inc. (2004) *MATLAB(R) The Language of Technical Computing*, 〈www.math works.com〉.

Wu, J.R., Li, Q.S. (2004) Finite Element Model Updating for a High-Rise Structure Based on Ambient Vibration Measurements, *Engineering Structures*, 26, pp.979~990.

Yang, Y.B., Chen Y.J. (2009) A New Direct Method for Updating Structural Models Based on Measured Modal Data, *Engineering Structures*, 31, pp.32~42.

Yi, J.H., Yun, C.B. (2004) Comparative Study on Modal Identification Methods using Output-Only Information, *Structural Engineering and Mechanics*, 17(3-4), pp.445~466.

Zhang, Q.W., Chang, C.C., Chang T.Y.P. (2000) Finite Element Model Updating for Structures with Parametric Constraints, *Earthquake Engineering and Structural Dynamics*, 29, pp.927~944.

Zhang, Q.W., Chang, T.Y.P., Chang, C.C. (2001) Finite Element Model Updating for the Kap Shui Mun Cable-Stayed Bridge, *Journal of Bridge Engineering*, 6(4), pp.285~293.

● 논문접수일 2010년 10월 11일
● 논문심사일 2010년 11월 4일
● 게재확정일 2010년 12월 6일